Congreso de Métodos Numéricos en Ingeniería 2009
Barcelona, 29 junio al 2 de julio 2009

HEAT TRANSFER ENHANCEMENT IN LAMINAR FLOW OF VISCOELASTIC FLUIDS THROUGH A RECTANGULAR DUCT

N. Peres[1]*, A. M. Afonso[2], M. A. Alves[2] and F. T. Pinho[1]

1: Centro de Estudos de Fenómenos de Transporte, Departamento de Engenharia Mecânica e Gestão Industrial
Faculdade de Engenharia da Universidade do Porto
Rua Dr. Roberto Frias s/n, 4200-465 Porto, Portugal
e-mail: noele.peres@gmail.com, fpinho@fe.up.pt web: http://www.fe.up.pt/~ceft

* Currently at Laboratoire de Modélisation en Mécanique et Procédés Propres, UMR 6181 CNRS- Université Paul Cézanne- Aix- Marseille III

2: Departamento de Engenharia Química, Centro de Estudos de Fenómenos de Transporte
Faculdade de Engenharia da Universidade do Porto
Rua Dr. Roberto Frias s/n, 4200-465 Porto, Portugal
e-mail: {mmalves,aafonso}@fe.up.pt web: http://www.fe.up.pt/~ceft

Keywords: free convection, viscoelastic fluids, rectangular duct, laminar flow

Abstract. *An investigation on convective heat transfer with viscoelastic fluids in a rectangular duct is carried out to analyze the influence of secondary flow on heat transfer enhancement on account of non-zero second normal-stress differences. The duct has an aspect ratio of 2, constant heat flux at the walls and the three dimensional numerical simulations use a finite-volume method. The numerical results are compared with the experimental heat transfer data of Hartnett and Kostic [1] and the influence of natural convection on the heat transfer process is also addressed. The viscoelastic fluid is described by the Phan-Thien-Tanner constitutive equation with non-zero second normal-stress difference ($N_2 \neq 0$). The simulations show an enhancement of heat transfer for viscoelastic fluids, quantified by increased levels of the local and mean Nusselt numbers. The origin of this enhancement is the fluid rheology, particularly the shear-thinning nature of the viscoelastic fluid and the existence of the secondary flow induced by the non-zero second normal stress differences. In addition, the correct prediction of the experimental results of Hartnett and Kostic [1], requires the inclusion of buoyancy, but this mechanism essentially distorts the secondary flow unless there are much larger temperature differences and/ or weaker second normal stress differences than tested. In the present simulations, buoyancy did not change the global heat transfer, but merely redistributed it, because the buoyancy-induced secondary flow was weaker than the Ψ_2- induced secondary flow. For these reasons, the effect of buoyancy decreases with an increase of N_2.*

1. INTRODUCTION

Heat transfer of some viscoelastic fluids in laminar flows in non-circular cross section ducts is characterized by a significant enhancement of the convection coefficient relative to the corresponding Newtonian fluid flows on account of the existence of secondary flows, as demonstrated experimentally by Hartnett and Kostic [1], who measured in a rectangular duct with an aspect ratio of 2. However, the corresponding increase in the viscous pressure losses is fairly small, i.e., the weak secondary flow has a larger influence upon the heat transfer behavior than on the fluid dynamics [1]. In fact, the earlier investigations of Wheeler and Wissler [2,3] had shown that neglect of secondary flow allowed accurate predictions of friction factor for viscoelastic fluids represented by a purely viscous constitutive equation (power law model), which consequently only considered rectilinear flow. Subsequently, Wheeler and Wissler [4] used an early optical diagnostic technique to measure velocity profiles and complemented these axial velocity measurements with calculations to infer the existence of a weak secondary flow as the cause of deviation of the measured profile from the profile for a rectilinear flow. Earlier, the existence of secondary flow of viscoelastic fluids in ducts of non-circular cross section had been theoretically predicted by Ericksen [5] and Green and Rivlin [6], according to Prager [7] and Wheeler and Wissler [4]. It is also worth mentioning that experiments conducted by Rao [8] in a rectangular duct with a larger aspect ratio of 5 confirmed the findings, but showed only an increase of 25% in the Nusselt number in contrast to the 100% increase reported by Hartnett and Kostic [1]. This difference was attributed to the larger aspect ratio reducing the strength of the secondary flow, but it is also important to refer the different thermal boundary conditions.

Secondary flows were directly measured by Laser-Doppler Anemometry by Gervang and Larsen [9] and also demonstrated to exist in their numerical calculations. Gervang and Larsen [9] and other authors [10-12] who predicted numerically the secondary flows, used a variety of constitutive equations: the Criminale-Eriksen- Filbey (CEF) model [9,10], the Reiner-Rivlin model [11] and the Phan-Thien- Tanner model [12]. All these calculations related the secondary motion in the duct cross-section with the magnitude of the second normal stress difference (N_2) of the viscoelastic fluids.

Investigations on heat transfer of viscoelastic fluid flows in rectangular ducts have also been carried out following the experiments of Kostic and Hartnett [1], but no attempt has really been made to predict quantitatively their experiments. Part of the problem lies actually with the lack of sufficient rheological data on the fluids used in those experiments. Gao and Hartnett [11] were probably the first to investigate systematically the heat transfer in this flow, relating the heat transfer enhancement with the intensity of second normal stress difference of the viscoelastic fluid which they represented with a Reiner-Rivlin model. Naccache and Mendes [13,14], Payvar [15] and Syrjälä [16] adopted the CEF rheological constitutive equation and again performed essentially qualitative simulations. It is worth emphasizing that Naccache and Mendes [13] initially considered forced convection and subsequently [14] extended their analysis to include free convection in a duct with two

vertical adiabatic walls and identical constant wall heat fluxes at the upper and lower walls. In [14] they reported various flow regimes depending on the relative magnitude of buoyancy and second normal stress difference effects. In particular, the authors observed a decrease in the magnitude of secondary flow when the second normal stress difference was large.

The rheological constitutive equations used so far in the numerical investigations of heat transfer enhancement in rectangular ducts are only valid in essentially viscometric flows, producing unphysical results in other flow conditions [17]. Hence, such features as flow unsteadiness, regions of extensional flow and separated flow, found in real situations, are not dealt with adequately by the CEF and the Reiner-Rivlin equations, which also lack memory effects. This sets the stage for our current investigation, where the aim is to use a constitutive model that is able to deal with a wide class of flows, possesses fading memory and behaves reasonably well under a variety of flow conditions. Additionally, we wish to reproduce the features measured by Hartnett and Kostic [1] and for that purpose the numerical simulations are carried out in the same geometry, a rectangular duct with an aspect ratio of 2. As is typical of many viscoelastic fluids, the flow is dynamically fully-developed, but is thermally developing, i.e., the Prandtl number of the fluid is very large, and the heat transfer fluxes are kept constant at all walls. The fluids tested are solutions of viscoelastic fluids, where the polymer contribution is described by a Phan-Thien — Tanner (PTT) rheological constitutive equation [18]. The heat transfer is investigated as a function of fluid rheology, especially to analyse the effect of the secondary flow strength, using the average and local Nusselt numbers. As will be demonstrated, the inclusion of free convection effects is essential to obtain numerical predictions that compare well with experimental heat transfer data. Note that the results in this conference paper are preliminary.

The calculations were carried out using an in-house code for viscoelastic fluid flow, which was modified by Nóbrega et al [19] to deal with the thermal energy equation, and was here improved to include free convection, a second order time stepping procedure and the high resolution scheme CUBISTA developed by Alves et al [20].

The paper is organized as follows: Section 2 presents the governing equations, the numerical method is briefly described in Section 3 and the validation of the implementation is presented in Section 4. Then, Section 5 analyses in detail the heat transfer in the rectangular duct flow of Newtonian and viscoelastic fluids and the paper ends with the main conclusions and an outline of future work in Section 6.

2. GOVERNING EQUATIONS

The governing equations required to solve for the flow and heat transfer of the PTT fluid are those for incompressible fluids with the PTT rheological constitutive equation, namely the conservation of mass,

$$\frac{\partial u_i}{\partial x_i} = 0 \tag{1}$$

the conservation of momentum,

$$\frac{\partial(\rho u_i)}{\partial t}+\frac{\partial(\rho u_j u_i)}{\partial x_j}=-\frac{\partial p}{\partial x_i}+\eta_s\frac{\partial^2 u_i}{\partial x_j\partial x_j}+\frac{\partial \tau_{ij}}{\partial x_j}+\rho g_i \tag{2}$$

and the conservation of thermal energy,

$$\frac{\partial(\rho cT)}{\partial t}+\frac{\partial(\rho c u_j T)}{\partial x_j}=\frac{\partial}{\partial x_j}\left(k\frac{\partial T}{\partial x_j}\right)+\eta_s\left(\frac{\partial u_i}{\partial x_j}+\frac{\partial u_j}{\partial x_i}\right)\frac{\partial u_i}{\partial x_j}+\alpha\tau_{ij}\frac{\partial u_i}{\partial x_j}+(1-\alpha)\frac{\tau_{jj}}{2\lambda}f(\tau_{ii}). \tag{3}$$

In the above equations u_i represents the velocity vector, p is the pressure, k is the thermal conductivity, c is the specific heat, ρ is the fluid density, t is the time, T is the fluid temperature and g_i is the acceleration of gravity vector. The fluid is represented as the sum of a Newtonian solvent contribution of viscosity η_s and a polymer contribution having an extra stress tensor τ_{ij}. The energy equation includes the effect of viscous dissipation by the Newtonian solvent as well as the two last terms on the right-hand-side, which account for the mechanical energy supply by the PTT fluid. The smaller term, which includes the viscous dissipation by the polymer, represents the entropic elasticity and quantifies the energy that is stored as entropy, i.e., that is dissipated thus contributing to temperature changes, whereas the contribution proportional to $(1-\alpha)$ is the energy elasticity quantifying the energy stored elastically as internal energy to be released later, therefore not contributing to temperature changes. The effect of α is fairly small, as demonstrated by Peters and Baaijens [21], but since we will be mostly concerned with fully-developed shear flow there will be no internal energy storage and only viscous dissipation matters, i.e., the two α terms will essentially cancel up and the final result will be mathematically equivalent to setting $\alpha=1$ [22,23]. However, in these preliminary calculations we did not include any effect of viscous dissipation in the thermal energy equation.

The evolution of the polymer stress tensor in a general nonisothermal flow is described by the complete form of the Phan-Thien— Tanner (PTT) rheological constitutive equation [23],

$$\phi(T)f(\tau_{kk})\tau_{ij}+\lambda\left[\frac{\partial\tau_{ij}}{\partial t}+u_k\frac{\partial\tau_{ij}}{\partial x_k}-\tau_{jk}\frac{\partial u_i}{\partial x_k}-\tau_{ik}\frac{\partial u_j}{\partial x_k}+\xi\left(\tau_{ik}S_{kj}+S_{ik}\tau_{kj}\right)\right]-\lambda\dot{H}_T\left(\tau_{ij}+\frac{\eta_p}{\lambda}\delta_{ij}\right)=\eta_p\left(\frac{\partial u_i}{\partial x_j}+\frac{\partial u_j}{\partial x_i}\right) \tag{4}$$

where λ is the fluid relaxation time, η_p is the coefficient of viscosity of the polymer, $S_{ij}\equiv\left(\partial u_i/\partial x_j+\partial u_j/\partial x_i\right)/2$ is the rate of deformation tensor and ξ is the constitutive parameter responsible for a non-zero second normal stress difference [24]. Note that coefficient ξ also affects other material properties, such as the shear viscosity and the first normal stress difference coefficient.

For the function $f(\tau_{kk})$, we adopted the linear stress coefficient form

$$f(\tau_{kk}) = 1 + \frac{\varepsilon\lambda}{\eta_p}\tau_{kk} \tag{5}$$

which is responsible for a shear-thinning viscosity and introduces coefficient ε that limits the extensional viscosity since this property is inversely proportional to ε for small ε and at high strain rates.

The last term on the left-hand-side of Eq. (4) accounts for the variation with temperature of the connector force that models the internal structure of the fluid in this constitutive equation. The term is zero for isothermal fluids, but following Peters and Baaijens [21] we also neglect this contribution. Finally, we also consider that all fluid properties are independent of temperature to simplify our analysis, even though it is known that in particular the viscosity coefficients and the relaxation time vary with temperature in a way that can be described by Arrehnius type expressions. By considering temperature independent properties the function that quantifies the time-temperature superposition principle, $\phi(T)$, is set to 1.

For the simulations with free convection, the last term on the right-hand-side of Eq. (2) must be considered. The variation of fluid density with temperature is dealt with in the classical manner, i.e., adopting the Boussinesq approximation. This means using Eq. (6) for the buoyancy term in the momentum equation and neglecting density variations elsewhere.

$$\rho g_i = \rho_0 g_i + \beta(T - T_0) g_i \tag{6}$$

In Eq. (6) β denotes the coefficient of thermal expansion and the subscript 0 denotes a reference temperature.

3. NUMERICAL METHOD

The governing equations (Eqs. 1-4) were solved using the in-house finite-volume method described in detail by Oliveira et al [25], here extended to deal with the energy equation, as explained below. Basically, the solution domain is decomposed into a set of adjacent control volumes over which those equations are integrated and then transformed into algebraic form. The discretized equations are solved sequentially for each dependent variable (u_i, p, τ_{ij}, T) using conjugate gradient solvers and the pressure field and pressure-velocity coupling are calculated following the SIMPLEC algorithm modified to deal with the stress-velocity coupling [25]. All diffusion terms are discretized with central differences, a second order scheme, the discretization of the advective terms relies on the high resolution scheme CUBISTA [20], a third order scheme in uniform meshes. For reasons of stability, the implementation of CUBISTA was carried out using the deferred correction approach, as explained in detail by Alves et al [26], and the non-linearities in

all equations are dealt with by iteration. The treatment of the full PTT model is explained in Afonso and Pinho [27].

For the mixed convection solutions the pressure is modified in the momentum equation to become a modified pressure p_m (with $p_m = p + \rho_0 g_i \left(x_i - x_{i,0} \right)$, where $x_{i,0}$ is a reference level), and the buoyancy force term ($\beta \left(T - T_0 \right) g_i$) is included in the source term of the corresponding algebraic equation. In terms of the algorithm outlined in Alves et al [26], within each iteration the thermal energy equation is the last to be solved, i.e., after the stress, velocity and pressure fields are computed.

4. VALIDATION AND NUMERICAL UNCERTAINTIES

The simulations of the flow and heat transfer in the rectangular duct were carried out first for pure forced convection and subsequently for mixed convection. For the validation and assessment of numerical uncertainty we follow the same approach and do it separately first for forced convection and afterwards for free convection. An assessment of the uncertainties of our code for isothermal flow of viscoelastic fluids has been carried out previously and extensively in a variety of flows [19, 26, 28], therefore we are here essentially concerned with the heat transfer results.

4.1. Flows with forced convection

The performance of the code in forced convection had been previously tested by Nóbrega et al [19] against a variety of analytical solutions: laminar flow in channels of Newtonian fluids under imposed wall heat fluxes and wall temperatures, using data from Shah and London [29], and channel flow for the simplified PTT fluid under imposed wall temperature [30] without and with viscous dissipation effects, both for fully-developed and thermally developing conditions. In all cases the predictions matched the analytical solutions to within 0.2% for thermal quantities and 0.4% for dynamical properties.

In addition, here we carried out a simulation in the rectangular duct flow of Hartnett and Kostic [1] for laminar Newtonian flow under conditions of pure forced convection, i.e., no free convection effects. This was achieved by considering the rectangular duct with adiabatic side and lower walls and heating the upper wall at a constant heat flux. The flow Reynolds number for this test case is Re^*=1113 and the Prandtl number is Pr^*= 6.4. The Reynolds and Prandtl numbers adopted follow the definitions introduced by Kozicki et al [31] for power law fluids given by Eqs. (7) and (8), respectively. In these equations, K and n represent the consistency and power indices of the power law, respectively. The adopted values of the coefficients a and b in equation (7) are for a rectangular duct of aspect ratio equal to 2. In the definition of the Peclet number of Eq. (8), α_t stands for the thermal diffusivity defined as $\alpha_t = k/(\rho c)$, where k and c denote the thermal conductivity and the specific heat of the fluid, respectively.

$$Re^* = \frac{\rho U^{2-n} D_h^n}{8^{n-1} K \left(\frac{a+bn}{n} \right)^n} \text{ with } a = 0.2440 \text{ and } b = 0.7276 \tag{7}$$

$$Pr^* = \frac{Pe}{Re^*} \text{ with } Pe = \frac{UD_h}{\alpha_t} \tag{8}$$

For the PTT fluid the equivalent definition to equation (7) is rather elaborate and requires a complex manipulation of the PTT equations as in [31] for various inelastic models. The use of a correct Reynolds number, equivalent to that of equation (7) for power law fluids, is essential in developing flows, but for fully-developed hydrodynamic and thermal conditions the Nusselt number becomes independent of the Reynolds number [29]. Since in this work our primary concern was precisely the prediction of heat transfer for fully-developed conditions, we defined the Reynolds number for PTT fluids using a simpler expression, namely $Re^*_{\text{PTT}} = \rho U D_h / \eta_0$, where $\eta_0 = \eta_P + \eta_s$ is the zero shear rate viscosity.

The flow physical domain is a rectangular duct with a height H of 9 mm and a width W of 18 mm, thus defining a hydraulic diameter $D_h =$ 12 mm. The length of the duct is L=533.33 D_h, x is the longitudinal coordinate, y and z are the vertical and spanwise directions, respectively and the duct inlet is located at x=0. For computational efficiency, depending on the symmetries of the heat transfer flow problem half or a quarter of the physical domain was mapped onto the computational domain. In the absence of free convection and when the upper and lower walls were heated the computational domain was a quarter of the physical domain because there were two symmetry planes, one in the spanwise direction (z) and the other in the transverse direction (y), hence the computational domain had a rectangular cross section with two planes of symmetry. When only the upper wall was heated the transverse direction symmetry plane no longer existed and the computational domain had to be half the physical domain and had now a square cross-section with one symmetry plane and three walls. In this case the number of cells was doubled in the y-direction, in order to keep the same cell sizes as in Table 1. Finally, the simulations with free convection were carried out with adiabatic side walls and heating at the lower and upper walls, which corresponds to a plane of symmetry in the physical domain at z/W=0.5 (or z/H=1). Here, the computational domain is again half of the physical domain and the mesh used is the same as in the previous case.

Three different uniform meshes were used as in Table 1, and the evolution of the local Nusselt number along the upper wall, averaged along z direction, is plotted in Figure 1 and compared with the corresponding experimental data of Hartnett and Kostic [1] and with the asymptotic fully-developed Nusselt number of 3.539 for a single wall heating, as listed in Shah and London [29]. This asymptotic value was obtained analytically

considering, as in their calculation, that the fluid properties are independent of temperature.

Henceforth, for the calculations of the flow and heat transfer in the rectangular duct to be reported in Section 5, meshes having the caracteristics of mesh A will be used. Prior to that the code was tested in a benchmark flow for free convection, as reported next.

Meshes	N_x	N_y	N_z	δ_x/D_h	δ_y/D_h	δ_z/D_h
A	800	10	20	0.667	0.0375	0.0375
B	1600	10	20	0.333	0.0375	0.0375
C	1600	15	30	0.333	0.025	0.025

Table 1- Mesh characteristics for the forced convection Newtonian flow in a rectangular duct (refers to one quarter of physical domain).

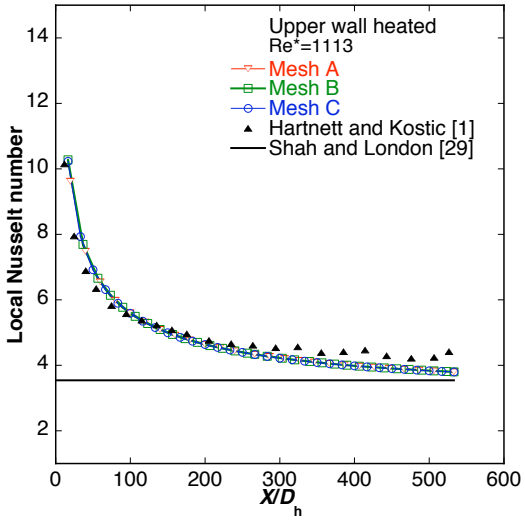

Figure 1- Variation of the local Nusselt number along the upper wall of the rectangular duct for laminar Newtonian flow.

4.2. Flows with free convection

To test the implementation of free convection, simulations were carried out for the benchmark case of Guo and Bathe [32] of flow of a Newtonian fluid inside a rectangular cavity having a ratio of width (W) over height (H) of 1:8. The fluid is initially at a relative temperature of 0°C, one side wall is set at +0.5°C and the other is set at -0.5°C, thus defining $\Delta\theta = 1°C$, while the upper and lower walls are adiabatic. Hence, the flow is driven exclusively by free convection effects and is such that the Rayleigh number $Ra = W^3\rho_0^2 c\|g_i\|\beta\Delta T/(\mu k) =$ 3.4 x 10^5 and the Prandtl number $Pr = \mu c/k =$ 0.71 (cf. [32] for all fluid properties and dimensions).

Guo and Bathe [32] have performed calculations using four different non-uniform meshes and their velocity and temperature profiles in the mid plane were similar for all the meshes. We used a single uniform mesh with 61 cells in the x- direction and 271 cells in

the y- direction, having a level of refinement intermediate to that of the first and second meshes of Guo and Bathe [32] in the x-direction and similar to meshes M1 - M3 in y-direction, as can be assessed in Table 2, where the characteristics of all meshes are compared.

Meshes	δ_x/W	δ_y/W
Our	0.016393	0.02952
M1 [32]	0.01725	0.02987
M2 [32]	0.01483	0.02987
M3 [32]	0.0125	0.02987
M4 [32]	0.005	0.01

Table 2- Mesh characteristics for the problem of free convection flow in a cavity.

Even though the flow in the cavity is periodic, at this centre plane the profiles are essentially steady in time as is well shown in Figure 6 of Guo and Bathe [32]. Considering this, we performed only a steady state calculation to compared our predictions with Guo and Bathe's [32] results. In Figure 2 we plot the calculated temperature and velocity profiles taken at the $y = H/2$ midplane and compare them with the corresponding profiles calculated by Guo and Bathe [32]. The corresponding temperature distribution contour map is also presented in Figure 2(c). All our predictions match very well the time-averaged numerical results of Guo and Bathe [32].

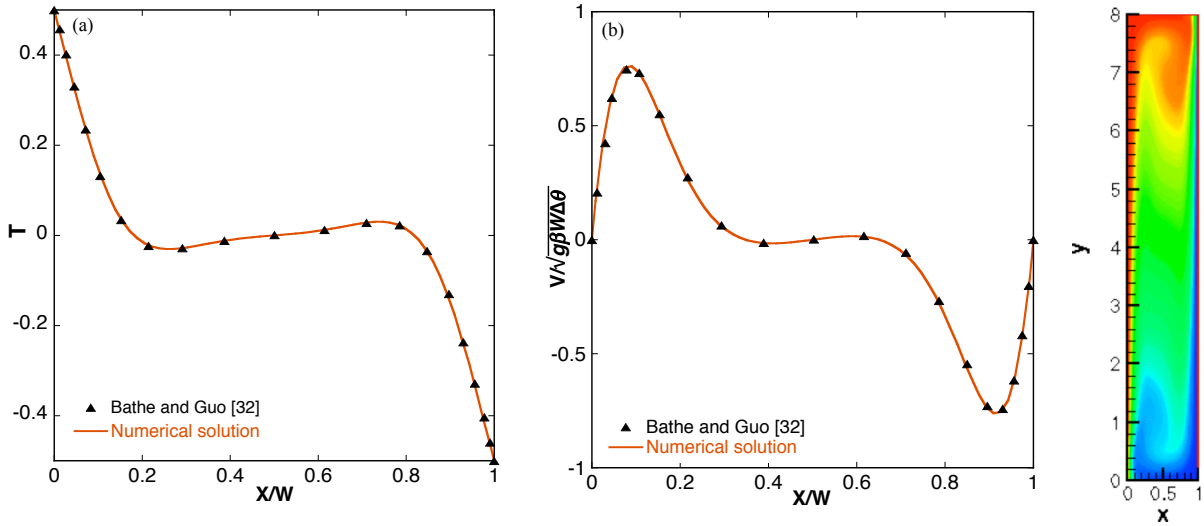

Figure 2- Flow in the benchmark cavity of Guo and Bathe [32]: (a) Temperature profile at $y= H/2$; (b) Velocity profile at $y= H/2$; (c) Temperature contour map.

5. RESULTS

5.1. Newtonian fluids

When free convection effects are minimised, as when only the upper wall is heated, Figure 1 shows that the flow and heat transfer calculations in the rectangular duct flow of Newtonian fluids match well the analytical solution and experiments. According to Shah and London [29], for fully-developed forced convection in the same rectangular duct the analytical value of the local Nusselt number is 4.12 when all the walls are heated, whereas we obtained Nu= 4.005 with mesh A, in another test case we carried out using a computational domain of a quarter of the physical domain.

If only the upper and lower walls are heated and the side walls are adiabatic, the fully-developed Nusselt number provided by Shah and London [29] is 5.2 (at both walls). This flow condition was measured by Hartnett and Kostic [1] and in Figure 3-a) we compare our predictions with their experimental data for water and the asymptotic value is Nu= 5.2. As we can see, our predictions without free convection cannot capture the correct behavior, but do capture the asymptotic behaviour of the analytical solution, also derived for pure forced convection. The comparison for the upper wall is not too bad since free convection effects there are significantly less intense than near the lower wall where the calculation misses the Nusselt number by more than 50%.

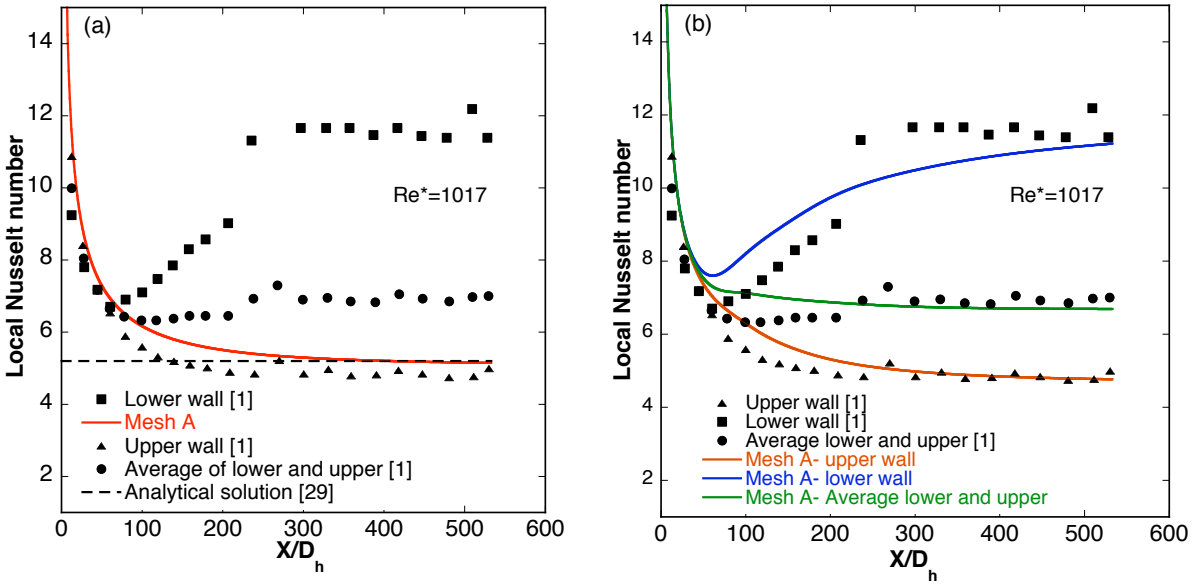

Figure 3- Variation of the local Nusselt number along a rectangular duct with heating at the upper and lower walls for water flow: (a) no free convection effects; (b) with free convection effects.

By repeating the calculation including free convection effects, the Newtonian measurements of Hartnett and Kostic [1] are essentially captured with minor

discrepancies, such as some data scatter and the sudden jump in the lower wall *Nu* profile, as can be assessed in the plot of Figure 3-b). Clearly, it is necessary to include the effects of free convection for an adequate prediction of the experimental measurement data.

5.2. Phan-Thien—Tanner fluid

The major problem in attempting to reproduce the experimental heat transfer data of Hartnett and Kostic [1] for non-Newtonian fluids is the lack of rheometric data in their paper for a complete characterization of the fluid. Hartnett and Kostic [1] only give data on the shear viscosity of their fluid, an aqueous solution of polyacrylamide (PAA, type Separan AP-273 from Dow Chemical Co.) at a concentration of 1000 wppm using Chicago tap water and nothing is said about the fluid elasticity properties, i.e., no data on the normal stress difference coefficients in shear flow or on the storage and dissipation moduli (*G*' and *G*") for small amplitude oscillatory shear flow.

We have fitted five different models to their viscosity data as plotted in Figure 4-a) using the parameters of Table 3, which includes the mean velocity required to obtain the same Reynolds number, but using the definition of Re^{*}_{PTT}, and the corresponding values of the flow Deborah number, which is defined here as $De = \lambda U / D_h$. In addition, we plot in Figures 4-b) and 4-c) the corresponding variation with shear rate of the first (Ψ_1) and second (Ψ_2) normal stress difference coefficients for the same model fluids.

Simulation	η_p [Pa·s]	η_s [Pa·s]	ξ	ε	λ[s]	U [m/s]	De
A	0.26	0.0055	0	0.25	5.0	0.80	333.33
B	0.26	0.0055	0.01	0.25	5.0	0.80	333.33
C	0.11	0.0055	0.01	0.25	0.5	0.80	33.33
D	0.11	0.0055	0.02	0.25	0.5	0.80	33.33
E	0.11	0.0055	0.03	0.25	0.5	0.80	33.33

Table 3- Parameters used for the PTT simulations.

There are essentially two different sets of fittings of the shear viscosity, one for models A and B and the other for models C, D and E. Models A and B, which predict $\Psi_2 = 0$ and $\Psi_2 \neq 0$, respectively, have stronger shear-thinning than Hartnett and Kostic's PAA solution. The curves for A and B are quite similar, since the value of ξ used in model B is fairly small and has a small effect on the viscosity, with model A slightly closer to the experimental data than model B at the high shear-rate end of the power law region. In spite of the negligible influence of ξ on the viscosity, this parameter has a non-negligible influence upon the heat transfer performance via Ψ_2 - induced secondary flow, as will be shown below. Essentially, the stronger shear-thinning of this set of models, relative to the experimental data, is characterized by flow curves below that data at the high shear-rate end of the power law region and above at the low shear rate edge. Another characteristic of these two models is that they predict well the first Newtonian plateau of viscosity. A

better fitting of the shear viscosity could be achieved only by using a multimode PTT model. However, by reducing significantly the zero-shear rate viscosity, as with models C, D and E, the viscosity fitting improves significantly at shear rates in excess of 1 s^{-1}, whereas below this value there is a large underprediction with a constant viscosity.

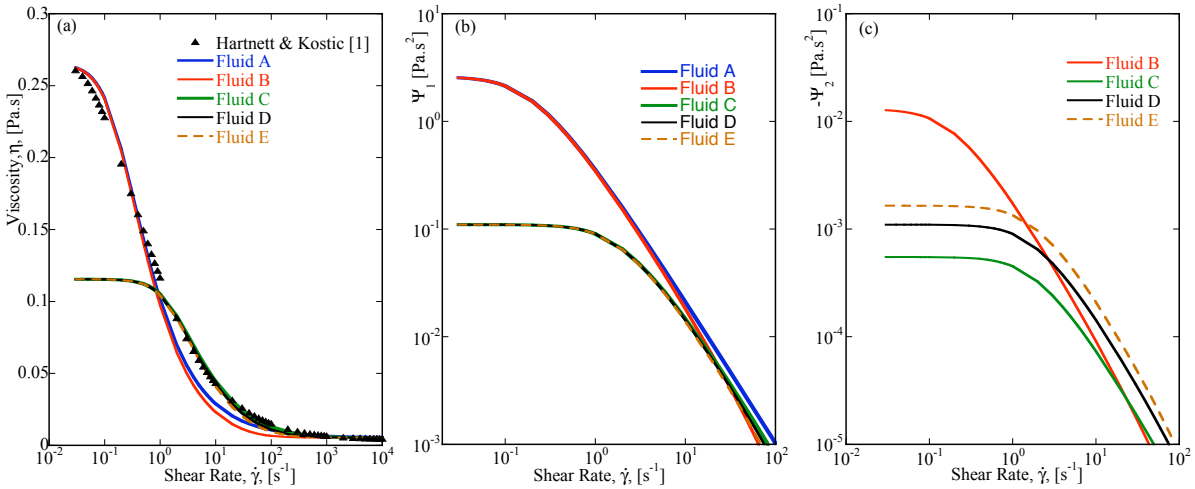

Figure 4- Rheology of the tested PTT solutions and comparison with Hartnett and Kostic [1] when available: (a) Shear viscosity; (b) Ψ_1; (c) - Ψ_2.

The performance of the five models in terms of first normal stress difference coefficient (Ψ_1) is plotted in Figure 4 (b). All the five models have shear-thinning behavior, with models A and B exhibiting the higher values of $\Psi_{1,0}$ (the limiting Ψ_1 value at zero shear rate), whereas models C, D and E have lower values of $\Psi_{1,0}$. The major influence of ξ on Ψ_1 is observed at large shear rates. The second normal stress difference coefficient is plotted in Figure 4 (c) as $-\Psi_2$. For model A, Ψ_2=0. For the other models, $-\Psi_2$ is circa two orders of magnitude lower than Ψ_1 and at high shear rates higher values of Ψ_2 correspond to higher values of ξ. Fluid B has a higher value of $\Psi_{2,0}$ (Ψ_2 at zero shear rate) in spite of having the lowest non-zero value of ξ, because Ψ_2 is also proportional to η. However, this occurs at low shear rates, when N_2 assumes small numerical values of little relevance, and likely to occur near the center of the duct. It will be confirmed later that in the center of the duct the secondary flow is very weak.

Calculations of flow and heat transfer in the rectangular duct for the PTT fluids were carried out first without buoyancy. The flow for model A is purely axial, but as soon as $\Psi_2 \neq 0$ a secondary flow becomes superimposed on the main flow, as can be seen in Figure 5, where the streamline projections for the secondary flow are plotted for model D. Gervang and Larsen [9] showed that the magnitude of the secondary-flow velocities are typically two orders of magnitude lower than that of the streamwise velocity, and depends on the values of both ξ and the Deborah number. This was also found to be true in our

calculations: for the simulation with model D the maximum secondary-flow velocities are close to 3 x 10^{-4} m/s for maximum streamwise velocities of about 0.8 m/s, i.e. the streamwise flow has velocities three orders of magnitude larger than the secondary flow. Similar results were obtained by Afonso and Pinho [27], who performed numeric calculations of square duct flow of PTT fluids and showed the increase of secondary flow strength with the value of ξ.

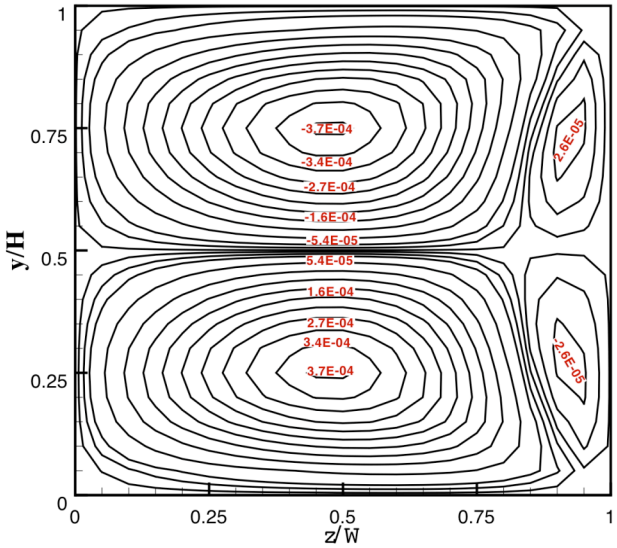

Figure 5- Projected streamlines of the secondary flow in the duct cross section corresponding to the case of model D in Table 3, without buoyancy. Half the geometry is shown. Values for secondary flow rate normalized by total axial flow rate.

In Figure 5 we show the projected streamlines of the secondary flow for half of the cross-section, when the flow is full-developed. For square ducts the secondary flow patterns are symmetric about the diagonal and the two mid planes, whereas when the aspect ratio increases the vortices expands near the top and bottom walls while squeezing them near the side walls [27], as in the present case. In addition to their size, the larger vortices are characterized by maximum flow rates which are one order of magnitude larger than those of the smaller vortices. Those two large vortices are responsible for refreshing the fluid near the upper and lower walls even though this secondary flow is weak by comparison with the main streamwise flow. Even though this secondary flow is weak, and has a negligible effect upon the friction it has a strong impact on the heat transfer because it continuously refreshes the fluid near the walls and contributes to fluid mixing, thus enhancing the Nusselt number. This effect is well shown in Figure 6-a), where the variation with *x* of the local Nusselt number is plotted for the various PTT flows and compared with the experimental data of Hartnett and Kostic [1] for their 1000 wppm PAA solution. The predicted Nusselt numbers increase with ξ (or Ψ_2), almost doubling between cases A and E and approaching the experimental behaviour. However, these predictions do not capture

the differences between lower and upper Nusselt numbers observed in the experiments, since the buoyancy effect was not simulated.

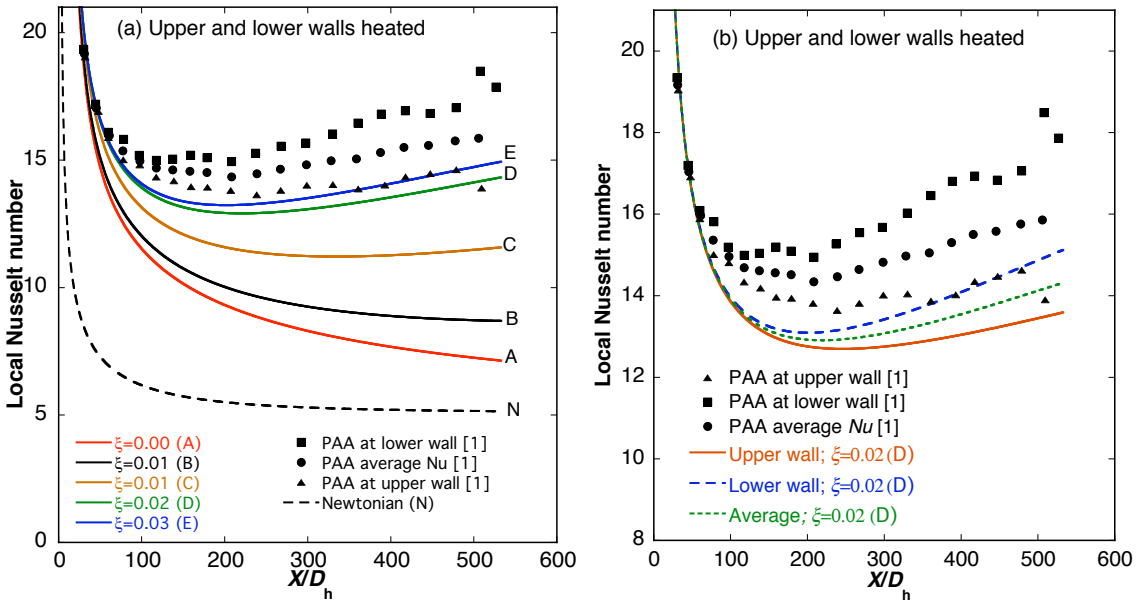

Figure 6- Variation of the local Nusselt number along a rectangular duct with heating at the upper and lower walls at Re^*= 1368: (a) forced convection (Newtonian flow at Re^*= 1017); (b) Mixed convection.

The dashed line (marked N) in Figure 6-a) pertains to the Newtonian forced convection prediction and shows that the enhancement of heat transfer is not exclusively due to the secondary flow. In fact, curves N for a Newtonian fluid and A for a PTT fluid do not have secondary flows, their differences being the Reynolds number (which at least for fully-developed conditions will have no impact at all) and fluid rheology. Whereas the Newtonian fluid has a constant viscosity, the PTT fluid is shear-thinning and this increases the flow shear rates near the wall. The consequence for the heat transfer, as explained in [30] is that the more plug-like shape of the PTT velocity profile (relative to that for the Newtonian fluid) leads to a higher proportion of flow rate near the wall, thus reducing the thermal resistance. The comparison between curves A and N also show a slower thermal development for the PTT fluid, in agreement with the findings of Coelho et al [30] for flow in pipes and channels.

By increasing the intensity of secondary flow (increasing ξ) the evolution of the Nusselt number also changes qualitatively: in the absence of or for weak secondary flow the Nusselt number continuously decreases towards an asymptotic value corresponding to the fully-developed thermal and hydrodynamic flow. When the intensity of secondary flow is increased the Nusselt number increases with x after an initial decrease to a minimum at about $x/D_h \approx 150$ to 300. This is seen both with the experimental data [1] and the predictions with the PTT model. It is important to keep in mind that there is a difference in Reynolds number which may justify some differences in developing flow conditions,

but not under fully-developed conditions. However, the difference between the Reynolds numbers is not so large as to justify the discrepancy of the Nusselt numbers we observe in Figure 6 (a).

The PTT flow of case D was calculated also including buyoancy effects and the corresponding longitudinal variation of the predicted Nusselt number is compared with the experimental data of Hartnett and Kostic [1] in Figure 6-b). Qualitatively, the trends measured by Hartnett and Kostic [1] are captured, but there is still a general underprediction and this could partially be due to a different definition of Reynolds number, an issue to be addressed later. A quantitative prediction will require further increases in parameter ξ and/ or the consideration of temperature dependent fluid properties, both of which we are currently investigating. It is also worth comparing the Newtonian and PTT results of Figures 3 and 6, respectively to conclude that buoyancy effects on heat transfer are less pronounced for the PTT fluid than for the Newtonian fluid. For a Newtonian fluid the lower wall Nusselt number is three times that at the upper wall, whereas for the PTT fluid that difference is an order of magnitude smaller at around 25% (this refers to fully-developed data or to data at the end of the computational domain). Presumably this is because the secondary flow induced by buoyancy for Newtonian fluids is rather weak near the upper wall and much stronger near the bottom wall. For the PTT and viscolastic fluids the secondary flow exists because $\Psi_2 \neq 0$ and this Ψ_2- induced flow is not affected by the wall temperature, i.e., it is identical near the upper and lower walls thus homogenizing the thermal behavior. In addition the Ψ_2-secondary flow is stronger than the secondary flow induced by buoyancy (for the present heat fluxes/ temperature differences) and for that reason there are also smaller differences between the Nusselt numbers at the lower and upper walls than for the Newtonian fluid, cf. in Figure 6 (a) and compare with Figure 3.

For the above reasons, the effect of buoyancy in this global heat condition is also expected to be less dramatic than for a Newtonian fluid. Whereas for a Newtonian fluid buoyancy is responsible for switched on the secondary flow, a mechanism for refreshing the fluid near the walls, with the viscoelastic fluids it merely changes and distorts the existing secondary flow, as shown in Figure 7 and by comparison with Figure 5. Naturally, this distortion by buoyancy is smaller the larger the strength of the Ψ_2- secondary flow and the smaller the temperature differences. Additionally, the contributions to the secondary flow of Ψ_2 and of buoyancy can be constructive or destructive, (the buoyancy driven secondary flow direction depends on the boundary conditions), so the final outcome is not necessarily predictable. What can be expected is that with the main effect being rheological, there is enhancement of heat transfer whenever Ψ_2 is increased and for fluids with $\Psi_2 = 0$ there is also enhancement associated with the shear-thinning character of the fluids, as was found by Coelho et al [30] and Pinho and Oliveira [33].

The comparison between Figures 5 and 7 confirms that buoyancy distorts the secondary flow pattern induced by Ψ_2, increasing the magnitude of the secondary flow for one large

and one opposite small vortex, while decreasing in similar proportions the magnitudes of the secondary flow in the other two vortices. In the end the total amount of secondary flow remains essentially unchanged, but there is a clear enhancement in its asymmetry. The comparison between Figures 5 and 7, without and with buoyancy, respectively, also confirms that the effect of free convection is smaller than the effect of Ψ_2 for case D, and this model has a small value of ξ.

Inspection of Figure 6 (b) and comparison with Figure 6 (a) shows that these changes in the cross section flow do not change the average Nusselt number, but differentiate the behaviour at the lower and upper walls. The lower wall Nusselt number becomes larger than the average value because secondary flow near the bottom wall was increased and the upper wall Nusselt number is decreased because the secondary flow in its vicinity is reduced, thus qualitatively approaching the calculated quantities to the measured quantities. However, for this particular case we do not really see an enhancement of the global heat transfer by including buoyancy effects.

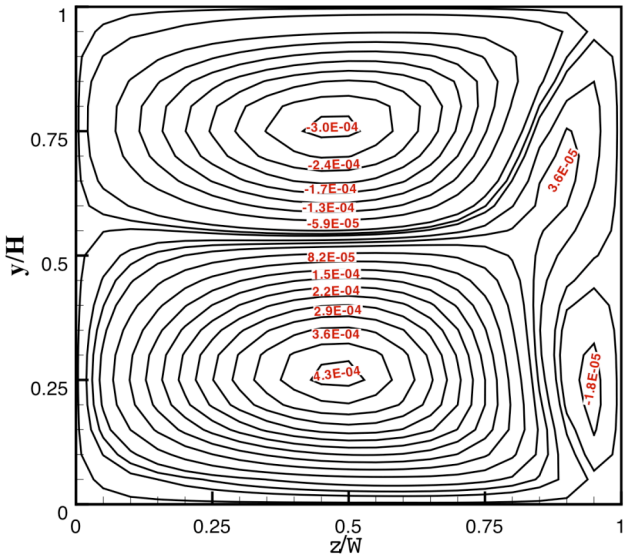

Figure 7- Projected streamlines of the secondary flow in the duct cross section corresponding to the case of model D in Table 3, with buoyancy. Half the geometry is shown. Values for secondary flow rate normalized by total axial flow rate.

6. CONCLUSIONS

A preliminary investigation of the flow and heat transfer characteristics of viscoelastic fluids described by the complete form of the Phan-Thien—Tanner constitutive equation in a rectangular duct has been carried out and compared with experimental data from Hartnett and Kostic [1]. These authors have reported the enhancement of heat transfer

associated with the existence of secondary flow due to fluid elasticity. We have shown numerically that such rheological features are fundamental for the enhancement, but are not the only cause, since part of the increased heat transfer comes from the shear-thinning viscosity of the fluid (although a smaller part than that due to Ψ_2).

This investigation has also shown that a quantitative capture of the measured data must necessarily include buoyancy effects to differentiate the heat transfer at the lower and upper walls. The underprediction of Hartnett and Kostic's data however, presumably stems from an insufficient level of secondary flow originating from a low Ψ_2, since the predictions for Newtonian fluids without and with buoyancy effects matched the experiments reasonably well, but can also be associated by a slower flow development given the different definitions of the Reynolds number used. However, we believe the issue of Reynolds number to be only a partial solution, since the use of model D did not change the numerical value of the Reynolds number by a large factor. In any case this issue should be addressed in the future. In addition, the preliminary numerical investigation of the buoyancy driven benchmark flow produced results that collapsed with those of Guo and Bathe [32], showing the correct numerical implementation of this mechanism.

This research continues aimed at improving the degree of agreement between the predictions and the experiments, which will require the use of higher values of parameter ξ and/or temperature dependent fluid properties and also a definition of the Reynolds number more in agreement with the definition used by Hartnett and Kostic [1]. As shown here, for fluids with a strong secondary flow induced by second normal stress effects, buoyancy will not enhance the global heat transfer, but essentially redistributes it. If the temperature differences involved are much larger it is possible that the effects induced by buoyancy will exceed those induced by the secondary normal stress differences and we will observe heat transfer enhancement due to buoyancy with viscoelastic fluids.

7. ACKNOWLEDGEMENTS

The authors would like to acknowledge financial support of FCT through projects PTDC/EME-MFE/70186/2006 and PTDC/EQU-FTT/70727/2006. AM Afonso wishes to thank FCT for support through his PhD scholarship SFRH/BD/28828/2006.

REFERENCES

[1] J. P. Hartnett and M. Kostic, "Heat transfer to a viscoelastic fluid in laminar flow through a rectangular channel", *Int. J. Heat Mass Transfer*. Vol. **28**, pp. 1147-1155, (1985).

[2] J. A. Wheeler and E. H. Wissler, "The friction factor- reynolds number relation for the steady flow of pseudoplastic fluids through rectangular ducts. Part I. Theory" *AIChEJ.* Vol. **11**, pp. 207-212, (1965).

[3] J. A. Wheeler and E. H. Wissler, "The friction factor- reynolds number relation for the steady flow of pseudoplastic fluids through rectangular ducts. Part II. Experimental results" *AIChEJ.* Vol. **11**, pp. 212-216, (1965).

[4] J. A. Wheeler and E. H. Wissler, "Steady flow of Non-Newtonian fluids in a square duct" *Trans. Soc. Rheol*. Vol. **10**, pp. 353-367, (1966).

[5] J. L. Eriksen, "Overdetermination of the speed in rectilinear motion of non-Newtonian fluids" *Quart. Appl. Math.* Vol. **14**, pp. 318-321, (1956).

[6] A. E. Green and R. S. Rivlin, "Steady flow of non-Newtonian fluids through tubes" *Quart. Appl. Math*. Vol. **14**, pp. 299-308, (1956).

[7] W. Prager, *Introduction to Mechanics of Continua*. Ginn and Co, Boston, (1961).

[8] B. K. Rao, "Laminar mixed convection heat transfer to viscoelastic fluids in a 5:1 rectangular channel" *Int. J. Heat Fluid Flow* Vol. **10 (4)**, pp. 334-338, (1989)

[9] B. Gervang and P. S. Larsen, "Secondary flows in straigth ducts of rectangular cross section" *J. Non-Newt. Fluid Mech.* Vol. **39**, pp. 217-237, (1991).

[10] P. Townsend, K. Walters and W. M. Waterhouse, " Secondary flows in pipes of square cross- section and the measurement of second normal stress difference" *J. Non-Newt. Fluid Mech*. Vol. **1**, pp. 107-123, (1976).

[11] S. X. Gao and J. P. Hartnett, " Heat transfer behavior of Reiner-Rivlin fluids in rectangular ducts" *Int. J. Heat Mass Trans*. Vol. **39**, pp. 1317-1324, (1996).

[12] S. - C. Xue, N. Phan-Thien and R. I. Tanner, " Numerical investigations of Lagrangian unsteady extensional flows of viscoelastic fluids in 3-D rectangular ducts with sudden contractions" *J. Non-Newt. Fluid Mech*. Vol. **37**, pp. 158-169, (1998).

[13] M. F. Naccache and P. R. Souza Mendes, "Heat transfer to non-Newtonian fluids in laminar flow through rectangular ducts" *Int. J. Heat Fluid Flow.* Vol. **17**, pp. 613-620, (1996).

[14] M. F. Naccache and P. R. Souza Mendes, "Mixed convection in the laminar flow of viscoelastic liquids through rectangular ducts" *J. Thermophysics Heat Trans*. Vol. **11**, pp. 98-104, (1997).

[15] P. Payvar, " Heat transfer enhancement in laminar flow of viscoelastic fluids through rectangular ducts" *Int. J. Heat Mass Trans*. Vol. **40**, pp. 745-756, (1997).

[16] S. Syrjälä, "Laminar flow of viscoelastic fluids in rectangular ducts with heat transfer: a finite element analysis" *Int. Comm. Heat Mass Trans*. Vol. **25**, pp. 191-204, (1998).

[17] R. I. Tanner, *Engineering Rheology*, Clarendon Press, Oxford, (1985)

[18] N. Phan-Thien and R. I. Tanner, "A new constitutive equation derived from network theory" *J. Non-Newt. Fluid Mech.* Vol. **2**, pp. 353-365, (1977).

[19] J. M. Nóbrega, F. T. Pinho, P. J. Oliveira and O. S. Carneiro, " Accounting for temperature-dependent properties in viscoelastic duct flows" *Int. J. Heat Mass Trans*. Vol. **47**, pp. 1141- 1158, (2004).

[20] M. A. Alves, P. J. Oliveira and F. T. Pinho, " A convergent and universally bounded interpolation scheme for the treatment of advection" *Int. J. Num. Meth. Fluids* Vol. **41**, pp. 47-75, (2003).

[21] G. W. M. Peters and F. P. T. Baaijens, "Modelling of non-isothermal viscoelastic flows" *J. Non-Newt. Fluid Mech.* Vol. **68**, pp. 205-224, (1997).

[22] P. Wapperom and M. A. Hulsen, "Thermodynamics of viscoelastic fluids: the temperature equation" *J. Rheology* Vol. **42**, pp. 999-1019, (1998).

[23] F. T. Pinho and P. M. Coelho, "Fully-developed heat transfer in annuli for viscoelastic fluids with viscous dissipation" *J. Non-Newt. Fluid Mech*. Vol. **138**, pp. 7-21, (2006).

[24] N. Phan-Thien, "A nonlinear network viscoelastic model" *J. Rheology* Vol. **22**, pp. 259-293, (1978).

[25] P. J. Oliveira, F. T. Pinho and G. A. Pinto, "Numerical simulation of non-linear elastic flows with a general collocated finite-volume method" *J. Non-Newt. Fluid Mech*. Vol. **79**, pp. 1-43, (1998).

[26] M. A. Alves, P. J. Oliveira and F. T. Pinho, "Effect of a high-resolution differencing scheme on finite-volume predictions of viscoelastic flows" *J. Non-Newt. Fluid Mech.* Vol. **92**, pp. 287-314, (2000).

[27] A. Afonso and F. T. Pinho "Numerical investigation of the velocity overshoots in the flow of viscoelastic fluids inside a smooth contraction" *J. Non-Newt. Fluid Mech*. Vol. **139**, pp. 1-20, (2006).

[28] M. A. Alves, P. J. Oliveira and F. T. Pinho, "Benchmark solutions for the flow of Oldroyd-B and PTT fluids in planar contractions" *J. Non-Newt. Fluid Mech*. Vol. **110**, pp. 45-75, (2003).

[29] R. K. Shah and A. L. London, *Laminar Flow Forced Convection in Ducts*. edited by Thomas F. Irvine, Jr. and James P. Hartnett, Academic Press, 1978.

[30] P. M. Coelho, F. T. Pinho and P. J. Oliveira "Fully developed forced convection of the Phan-Thien—Tanner fluid in ducts with a constant wall temperature" *Int. J. Heat Mass Transfer.* Vol. **45**, pp. 1413-1423, (2002).

[31] W. Kozicki, C. H. Chou and C. Tiu "Non-Newtonian flow in ducts of arbitrary cross-sectional shape" *Chem. Eng. Sci.* Vol. **21**, pp. 665-679, (1966).

[32] Y. Guo and K. J. Bathe, "A numerical study of a natural convection flow in a cavity" *Int J. Num. Meth. Fluids*. Vol. **40**, pp. 1045-1057, (2002).

[33] F. T. Pinho and P. J. Oliveira, "Analysis of forced convection in pies and channels with the simplified Phan-Thien— Tanner fluid" *Int. J. Heat Mass Transfer.* Vol. **43**, pp. 2273-2287, (2000).